Asian Journal of Chemistry; Vol. 35, No. 9 (2023), 2247-2255

ASIAN JOURNAL OF CHEMISTRY

https://doi.org/10.14233/ajchem.2023.28226

Antifungal Activity of ZnO Nanobullets against *Schizosaccharomyces pombe*

BANDITA MOHAPATRA

University School of Biotechnology, Guru Gobind Singh Indraprastha University, Dwarka, New Delhi-110078, India

Corresponding author: E-mail: bmohapatraipu@gmail.com

Received: 25 June 2023; *Accepted*: 3 August 2023; *Published online*: 31 August 2023; AJC-21372

In this study, an enhanced antifungal response of ZnO nanobullets (NBs) against *Schizosaccharomyces pombe* is reported. The ZnO NBs were prepared by alkali precipitation method and confirmed by microscopic, morphological and optical studies using SEM, EDX, TEM, HRTEM and photoluminescence (PL) spectroscopic techniques. Growth kinetics and MIC studies were conducted following the growth inhibition percentage studies. Colony forming assay, well diffusion, disc diffusion, N-acetyl cysteine (NAC) effect on *S. pombe* growth, trypan blue study, cellular reactive oxygen species (ROS) quantification using H_2DCFDA dye, Bradford assay, DNA fragmentation and all other relevant protocols were performed in antifungal studies. ZnO nanobullets (NBs) were shown by SEM and TEM examinations to have an average size of 50 nm. The hexagonal wurtzite structure of ZnO NBs was confirmed by HRTEM's lattice fringe findings. Defect-related visible emissions at 412, 436, 457 and 564 nm were confirmed *via* PL analysis. It was found that ZnO NBs resulted in complete growth inhibition of *S. pombe* at 200 µg/mL. When *S. pombe* was treated with ZnO NBs, the Bradford assay revealed enhanced protein leakage, but the TBARS assay revealed lipid peroxidation brought on by reactive oxygen species (ROS). When *S. pombe* was exposed to ZnO NBs, the H_2DCFDA assay revealed increased ROS generation, whilst the trypan blue assay revealed increased cell membrane fusion and lower viability. According to present study, the treatment with ZnO NBs caused *S. pombe* to develop damaged cell walls, leaky proteins and DNA breakage.

Keywords: ZnO, Nanobullets, Antifungal activity, *Schizosaccharomyces pombe*.

INTRODUCTION

Emergence of multi-drug resistance in human and plant pathogenic fungi originating from the unregulated usage and reduced efficacy of antibiotics poses serious health and economic challenges for the mankind [1,2]. Infectious fungal diseases caused by human pathogenic fungi that exhibit multi-drug resistance are becoming very difficult to treat and have led to increasing morbidity and mortality in immuno compromised patients [3-5]. Emergence of resistance to the conventional fungicides in plant pathogenic fungi has led to deterioration of quality of crops and fruits resulting in huge production loss and heavy economic loss. Thus, there is a serious and urgent need to develop novel broad-spectrum antifungal agents for controlling and preventing fungal infections by adopting different strategies including usage of inorganic nanomaterials [6-12], antimicrobial peptides [13], *etc*. In recent years, nanoparticles of inorganic materials such as metals and metal oxides have been the focus of various studies due to their exciting physico-chemical properties as well as improved interaction with the membrane of microbes [14,15].

Nanoparticles of inorganic materials (*viz.* ZnO, Cu, Ag, CuO, Cu_2O, Fe_3O_4) have been found to exhibit good antifungal activity and have emerged as promising alternative for the control and treatment of various fungal infections [6-12,14-29]. Among the nanostructured metal oxide semiconductors, ZnO nanoparticles have attracted immense attention as an emerging antimicrobial due to their higher stability, low cost and longer shelf-life and good antimicrobial activity [30]. Recently, nanoparticles of ZnO were shown to cause growth inhibition of pathogenic plant fungi *Botrytis cinerea* and *Penicillium expansum* [21]. Dimkpa *et al*. [22] reported that 500 µg/mL of ZnO nano-particles inhibited growth of the pathogenic fungus, *Fusarium graminearum,* whereas Li *et al.* [23] demonstrated the antifungal action of ZnO nanoparticles against filamentous pathogenic fungus, *Sclerotinia homoeocarpa*, limiting its growth at a concentration of 400 µg/mL. Though there are several studies reporting antifungal response of ZnO nano-

particles, the understanding of the molecular processes is still unclear. Several mechanisms have been proposed to contribute towards the antifungal action of ZnO nanoparticles, including (i) production of ROS, (ii) intracellular oxidative stress generation due to the generated ROS, (iii) release of Zn^{2+} ions from ZnO nanoparticles, (iv) internalization of ZnO nanoparticles, (v) disintegration of cell membrane, (vi) leakage of protein and cellular material and (vii) DNA damage [20,25,30,31]. ZnO nanoparticles are known to produce ROS *viz.* singlet oxygen, superoxide radicals, hydroperoxyl radicals, hydroxyl radicals and H_2O_2. ROS is known to target cellular compounds and the complex lipid molecules in the cell membrane [20] and leads to lipid peroxidation [32]. Lipovsky *et al.* [30] used histidine to scavenge the generated ROS and demonstrated that ROS plays a role in the antifungal response of ZnO nanoparticles towards pathogenic *Candida albicans*. However, more studies are required to provide insight into the origin of strong antifungal response of nanostructured ZnO. The potent antibacterial properties of chemically produced ZnO nanobullets have been previously reported [33].

Though the antifungal properties of ZnO nanoparticles on different yeasts have been investigated [34], there are no reports on the effect of nanostructured ZnO on *S. pombe* till date. Present results demonstrated that ZnO NBs fully inhibited growth of *S. pombe* at 200 µg/mL. The results show that ROS production is crucial in determining the antifungal effect of ZnO NBs.

EXPERIMENTAL

The zinc oxide (ZnO) nanoparticles were prepared using $Zn(CH_3COO)_2{\cdot}2H_2O$ (SRL, India) and KOH (SDFCL, India).

Synthesis of ZnO nanobullets: The ZnO nanobullets were prepared by alkali precipitation method as described previously [33]. Briefly, 200 mM KOH was added dropwise to 200 mL aqueous solution of 20 mM $Zn(CH_3COO)_2{\cdot}2H_2O$ under stirring for 30 min to reach a final pH of 10. After 2 h, centrifugation was done to recover the precipitates followed by washing and drying at 80 ºC.

Characterization: The microstructure and morphology of the sample was analyzed using SEM (ZEISS), TEM, HRTEM and EDX (TECNAI G2 20, FEI). The photoluminescence (PL) spectroscopy was carried out using Edinburgh Instruments under 350 nm excitation.

Growth kinetics: The impact of ZnO nanobullets (NBs) on the growth kinetics of *S. pombe* was evaluated as per reported method [35]. Briefly, absorbance at 600 nm of the different *S. pombe* cultures grown at 32 ºC with shaking was monitored at a 2 h interval. Three independent biological studies were undertaken and the averages with S.D. were plotted.

MIC studies: To calculate the minimum inhibitory concentration (MIC), YE-agar plates with different ZnO NBs concentrations were prepared and *S. pombe* culture was plated on them. The plates were then incubated for 36 h at 32 ºC and the experiments were carried out three times.

Growth inhibition percentage studies: Colony counting method [36] was employed to estimate the percent growth inhibition of *S. pombe* treated with ZnO NBs. The percentage growth inhibition (I%) was calculated with respect to the untreated cells (control) using eqn. 1:

$$\text{Growth inhibition (\%)} = \frac{A_c - A_t}{A_c} \times 100 \quad (1)$$

where A_t = mean colony number in treated cells and A_c = mean colony number in the control.

Colony forming assay: *S. pombe* was grown overnight in YE media at 32 ºC with shaking. This overnight grown *S. pombe* culture was diluted to an absorbance of 0.3 at 600 nm the next day and subsequently allowed to grow till absorbance of 0.6 was reached at 600 nm. ZnO NBs (25, 50, 75, 100, 150 or 200 µg/mL) were mixed with the yeast cultures and the cultures were incubated at 32 ºC for 2 h. The cultures after 1/10 consecutive dilutions were spotted onto agar plates and incubated at 32 °C for 36 h and pictures of the plates were recorded. The experiments were conducted three times.

Well diffusion studies: *S. pombe* (100 µL, 2×10^7 cells/mL) was spread on YE-agar plates in which wells were made and 25, 50, 75, 100, 150 or 200 µg/mL of the ZnO NBs was put into the wells. This study was also conducted three times.

Disc diffusion studies: *S. pombe* (100 µL, 2×10^7 cells/mL) was spread onto the agar plates. After that, paper discs (Whatman, dia. 6 mm) with 25, 50, 75, 100, 150 or 200 µg/mL of ZnO NBs were kept on these plates. Similarly, Whatman paper discs (dia. 6 mm) loaded with 25, 50, 75, 100, 150 or 200 µg/mL of the common antibiotic, geneticin, were kept on agar plates on which *S. pombe* culture was plated.

Effect of *N*-acetyl cysteine (NAC) on *S. pombe* growth: The effect of NAC on the growth of *S. pombe* was checked as described previously [35]. Briefly, an absorbance at 600 nm of *S. pombe* cultures was adjusted to 0.1 and 200 µg/mL of ZnO NBs was added to them, followed by addition of different concentrations of NAC. The controls (i) cells with no NBs and no NAC, (ii) cells treated with 50 mM NAC and (iii) cells treated with only 200 µg/mL of ZnO NBs, were used. The kinetics of growth of yeast was evaluated by measuring $O.D._{600\ nm}$ after every 2 h. Three studies were undertaken and the average $O.D._{600\ nm}$ values with S.D. were noted.

Trypan blue assay: ZnO NBs (200 µg/mL) were added to mid-log phase *S. pombe* culture followed by growth of *S. pombe* at 32 ºC with shaking for 2 h. The culture was first pelleted followed by washing of the cell pellet with 1X PBS (pH 7.2), addition of trypan blue (0.1%) and incubation of 10 min. A suspension (1 µL) was mounted on the slides and analyzed under the microscope. The staining was done in 2 replicates (biological) with 3 replicates (technical) and 200 cells were analyzed in each technical replicate.

Quantification of cellular ROS using H_2DCFDA dye: Exponentially grown *S. pombe* was treated with either 10 mM H_2O_2 (control) or 200 µg/mL of ZnO NBs and incubated at 32 ºC for 2 h with 200 rpm shaking. After the treatment, the cultures were pelleted, followed by washing of the cell pellets with 1X PBS (pH 7.2) and addition of 5 µL H_2DCFDA dye was added. The cell suspension was then incubated in dark for 1 h and then washed twice. Pellets were resuspended, following which the suspension (1 µL) was placed onto glass slides. Imaging of

cells was done with plan apochromat 100X objective (oil) of the Nikon Eclipse Ni Light microscope. The cell periphery was marked in each cell, the mean adjusted fluorescence was quantified, integrated density with background reading was measured using ImageJ software. Quantification of the fluorescence intensity was done using ImageJ software from 200 cells for each sample [37,38]. Two independent measurements were undertaken with two technical replicates. Each sample (200 cells) were analyzed in each technical replicate and the average value of adjusted mean fluorescence of *S. pombe* was plotted with S.D.

Bradford assay: ZnO NBs (200 µg/mL) were added to log-phase *S. pombe* followed by incubation at 32 ºC for 2 h. Subsequently, Bradford assay analysis was undertaken using the standard protocol [39] to determine the concentration of protein in supernatants in the untreated *vs.* ZnO NBs treated samples. Average values from three independent experiments (with two technical replicates each) have been plotted with S.D.

DNA fragmentation studies: ZnO NBs (200 µg/mL) was added to mid-log phase grown *S. pombe* cells. These cultures were further incubated for 10 or 15 h at 32 ºC. Subsequently, isolation of genomic DNA from 200 µg/mL of ZnO NBs treated and untreated yeast cultures was done as per reported protocol [40] followed by agarose gel electrophoresis of the isolated genomic DNA.

RESULTS AND DISCUSSION

Morphology and microstructure studies: SEM and TEM techniques were used to analyze the wet chemically synthesized ZnO nanobelts (NBs) sample for morphology and microstructure. Since, size and shape are known to have an effect on the antifungal activities of ZnO nanostructures, this investigation was carried out [41]. The SEM images displayed in Fig. 1a-b reveal nanostructures with nanobullet-like morphology.

TEM image (Fig. 2a) clearly reveals the nanostructures with nanobullet-like morphology. HRTEM image from a nanobullet is presented in Fig. 2b, which shows fringes with lattice spacing of 2.48 Å confirming hexagonal wurtzite ZnO. The EDX spectrum (Fig. 2c) shows Zn, O atoms from ZnO nanobullets, whereas Cu is from the grid used. The width of these nanobullets was found as 50 nm (Fig. 2d) and the growth mechanism is reported earlier [33].

Photoluminescence studies: Photoluminescence (PL) spectrum from the sample is acquired under 350 nm excitation is presented in Fig. 3. The deconvolution reveals four peaks at 412, 436, 457 and 564 nm and these emissions were due to the defects such as zinc vacancies, zinc interstitials, oxygen interstitials, oxygen vacancies and other defects in ZnO [42]. The peak at 412 nm originates from transition from the conduction band (CB) to oxygen interstitial level [43]. An emission at 436 nm is attributed to the transition from Zn interstitials (Zn_i) to the acceptor level due to Zn vacancies [44,45], whereas emission at 564 nm is due to the transition from Zn_i to oxygen vacancy (O_v) level, whereas the peak at 457 nm is ascribed to transition between the Zn interstitial and oxygen interstitial [43].

ZnO nanobullets inhibit the growth of *S. pombe*: Present study aimed to examine the potential inhibitory effects of ZnO nanoparticles on the development of *S. pombe*. To investigate this phenomenon, the growth curve analyses on *S. pombe* in the presence or absence of ZnO nanobullets (NBs) at various doses were conducted. The growth curves clearly show that variation in the concentration of ZnO NBs from 25 to 150 µg/mL led to increasing growth inhibition of *S. pombe* (Fig. 4a). Moreover, a concentration of 200 µg/mL led to complete growth inhibition of *S. pombe*. To further examine the growth inhibition potential of ZnO NBs, the colony forming ability of *S. pombe* was checked without or with ZnO NBs. Cell viability of *S. pombe* was shown to decrease from 25 to 200 µg/mL of ZnO NBs when compared to untreated cells (Fig. 4b).

Next, in order to determine the MIC of ZnO NBs at which fission yeast failed to germinate on YE agar. Thus, *S. pombe* cells were plated on YE agar plates containing varying concentrations of ZnO NBs (25, 50, 75, 100, 150 or 200 µg/mL). As observed in Fig. 4c, *S. pombe* growth was completely inhibited at 200 µg/mL of ZnO NBs, which is consistent with the results

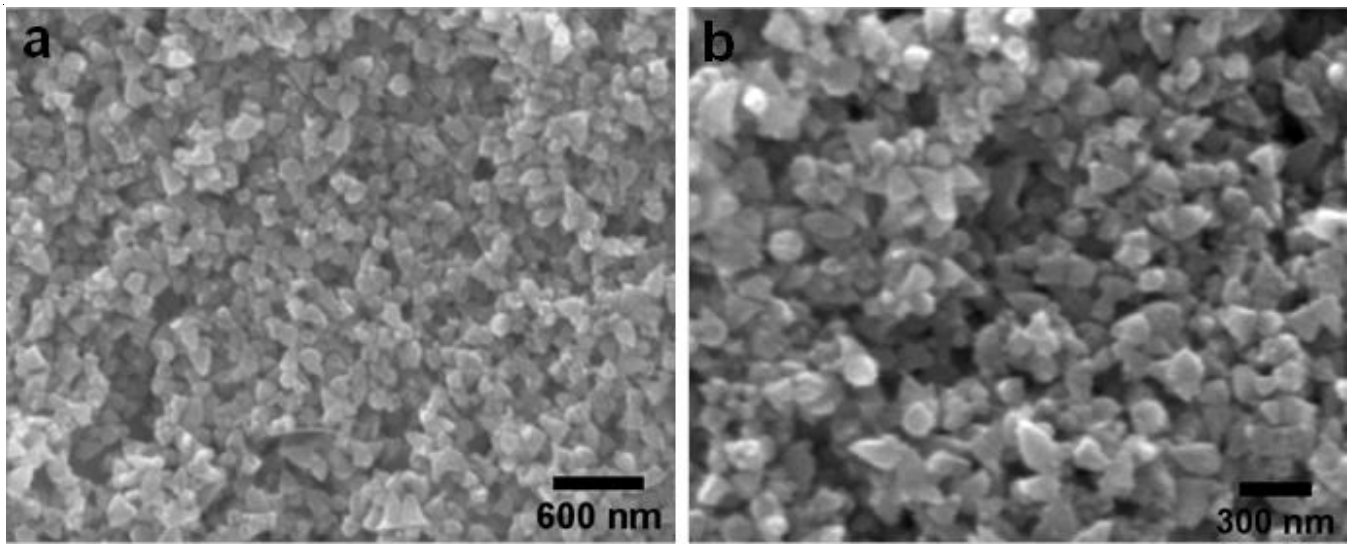

Fig. 1. SEM images of prepared ZnO nanobullet

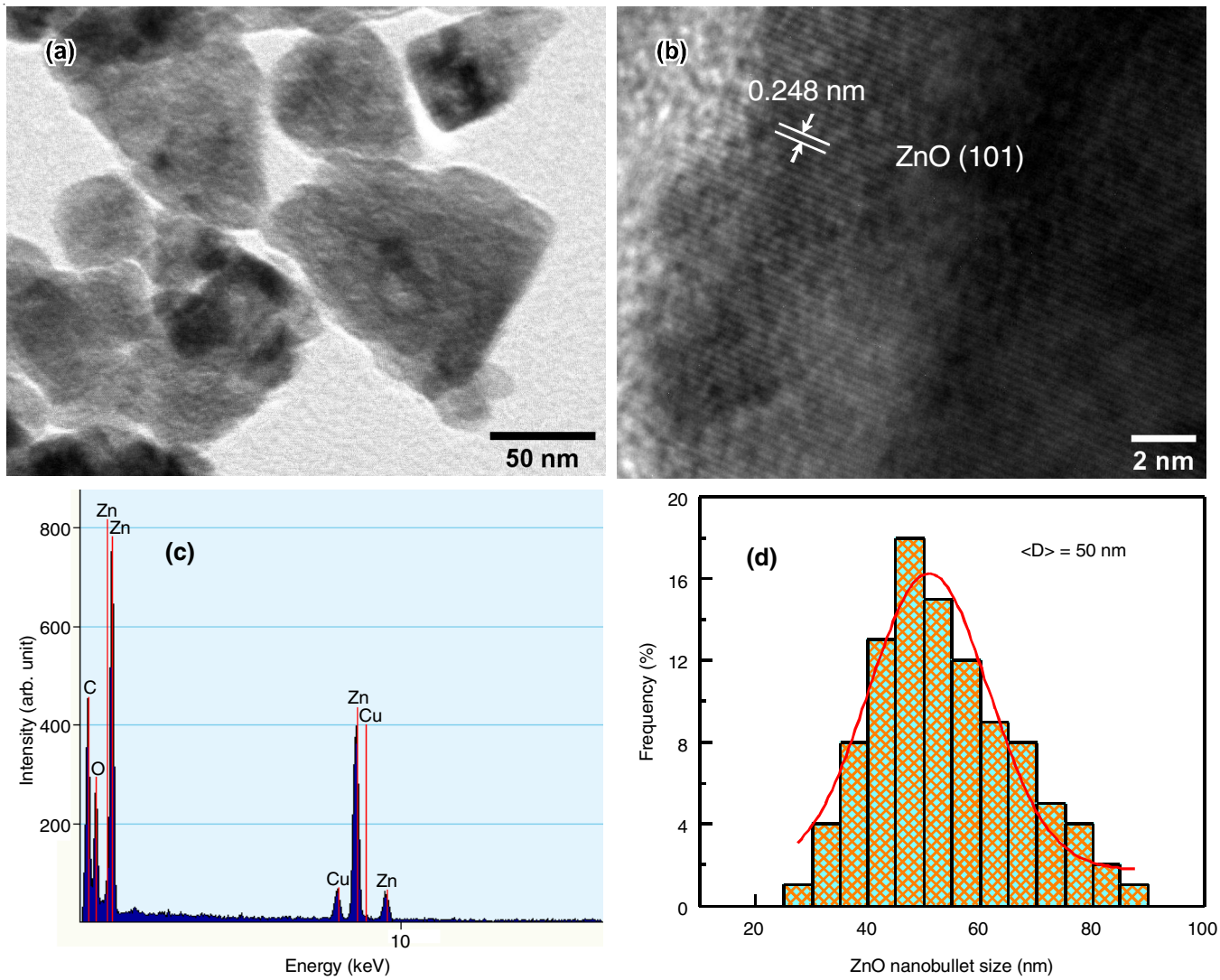

Fig. 2. (a) TEM image, (b) HRTEM micrograph, (c) EDX spectrum and (d) size distribution of ZnO nanobullets

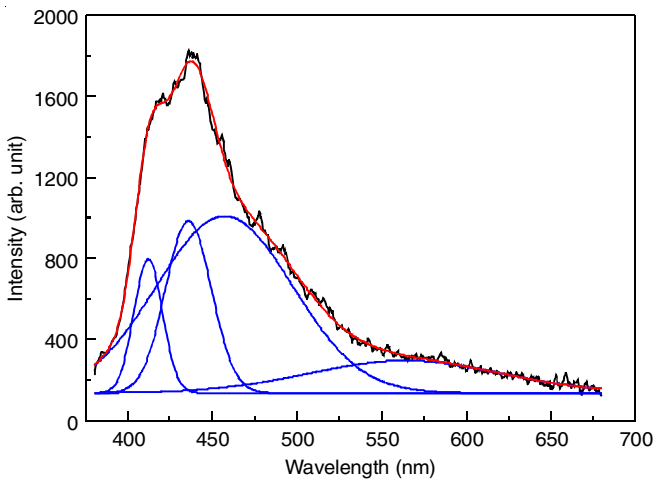

Fig. 3. Photoluminescence (PL) spectrum from ZnO nanobullets

of growth curve studies and colony forming assay. Compared to the reported MIC of ZnO nanoparticles (500 mg/mL) for inhibiting the growth of *Fusarium graminearum* [22], the MIC of ZnO NBs against *S. pombe* is significantly lower. The growth inhibition percentage at various concentration of ZnO NBs was also calculated and plotted (Fig. 4d). The growth inhibition percentage increased from 25.57 ± 3.13% to 99.53 ± 0.32% as the ZnO NBs concentration varied from 25 to 200 µg/mL. Subsequently, a comparative analysis was conducted between the aforementioned findings with the reported investigations (Table-1) related to various ZnO nanoparticles and their efficacy against a range of human and plant pathogenic fungi [17-27]. ZnO NBs are found to have better antifungal action with lower MIC, suggesting its potential as an exciting candidate for various applications.

To carry out the well diffusion assay, wells were bored into the plates on which *S. pombe* cells were plated. The zone of inhibition (ZOI) of ZnO NBs was found to be 11 ± 1, 13.7 ± 0.6, 17.7 ± 0.6, 20.3 ± 0.6, 24.3 ± 1.1 and 28 ± 2 mm at 25, 50, 75, 100, 150 and 200 µg/mL of ZnO NBs, respectively (Fig. 5a). The disc-diffusion assay also revealed the similar findings, showing that the ZOI grew together with the concentration of ZnO NBs. As shown in Fig. 5b, the ZOI of ZnO NBs against *S. pombe* was measured to be 12.3 ± 0.6, 15.3 ± 0.6, 16.8 ± 0.3, 18.3 ± 0.6, 19.8 ± 0.8 and 21 ± 1 mm at 25, 50, 75, 100, 150

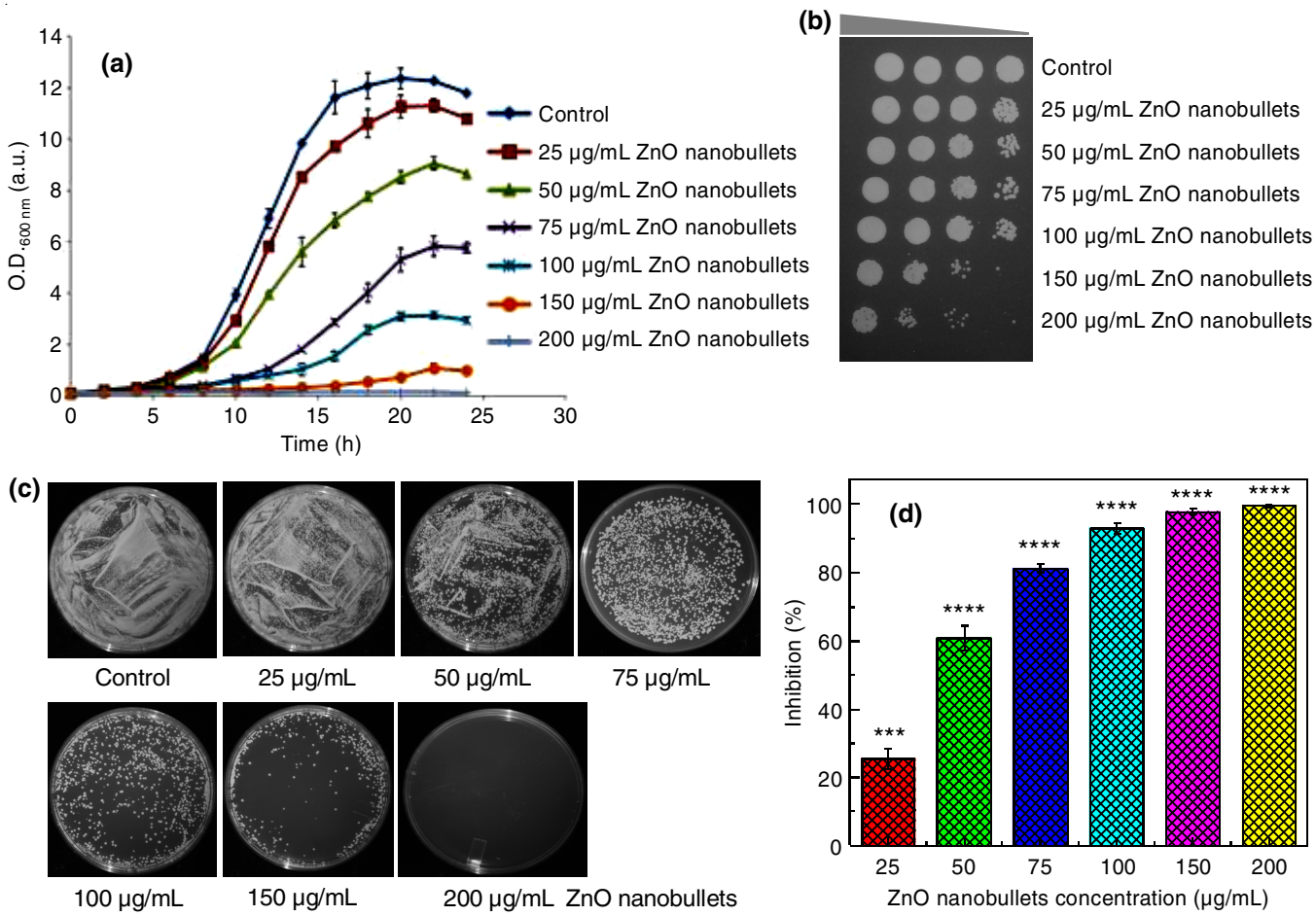

Fig. 4. (a) Growth curves of *S. pombe* in the presence or absence of ZnO NBs at different concentrations. (b) Results of colony forming assay of untreated or *S. pombe* cells treated with ZnO NBs at different concentrations. (c) Determination of MIC for ZnO NBs against *S. pombe*. (d) Percentage growth inhibition at different concentrations of ZnO NBs. Three separate experiments were undertaken and the averages with SD have been plotted. *p*-values (**** = $p < 0.0001$, *** = $p < 0.001$) estimated using Student's t test have been included

TABLE-1
COMPARATIVE ANTIFUNGAL ACTIVITIES OF ZnO NANOPARTICLES

Name of fungi	Antifungal agent	Synthesis method	MIC (µg/mL)	Ref.
Colletotrichum gloeosporioides	ZnO nanoparticles	Precipitation	312	[17]
Rhizoctonia solani	ZnO nanoparticles	Green synthesis	1000	[18]
Aspergillus niger	ZnO nanoparticles	Precipitation	2500	[19]
Candida albicans			5000	
Candida krusei	ZnO nanoparticles (40-75 nm)	Precipitation	500	[20]
Botrytis cinerea	ZnO nanoparticles (~ 70 nm)	Purchased from Alfa Aesar	976.56	[21]
Penicillium expansum			976.56	
Fusarium graminearum	ZnO nanoparticles	Purchased from Sigma-Aldrich	500	[22]
Sclerotinia homoeocarpa	ZnO nanoparticles	US Research Nanomaterials Inc	400	[23]
Fusarium oxysporum	ZnO nanoparticles	Precipitation	1600	[24]
Erythriciumsalmonicolor	ZnO nanoparticles	Sol-gel method	732.42	[25]
Candida albicans	ZnO nanoparticles (< 100 nm)	Purchased from Sigma-Aldrich	160	[26]
Saccharomyces cerevisiae	ZnO nanoparticles (50-70 nm)	Purchased from Sigma-Aldrich	1500	[27]
Schizosaccharomyces pombe	ZnO nanobullets	Precipitation	200	Present study

and 200 µg/mL, of ZnO NBs respectively in the disc diffusion assay. Using the disc diffusion method, the antifungal activity of ZnO NBs against *S. pombe* and geneticin was also examined. The ZOI of geneticin was found to be 13.3 ± 0.6, 16.3 ± 1.1, 18.7 ± 0.6, 21 ± 1, 24.7 ± 0.58, 29.3 ± 1.1 mm against *S. pombe* at 25, 50, 75, 100, 150 and 200 µg/mL of geneticin, respectively (Fig. 5c). These results confirmed the strong antifungal action exhibited by ZnO NBs against *S. pombe*, which are comparable to that of the widely used common antibiotic geneticin making it promising for future applications.

SEM analysis was carried out to investigate whether ZnO NBs treatment results in any change in the morphology and

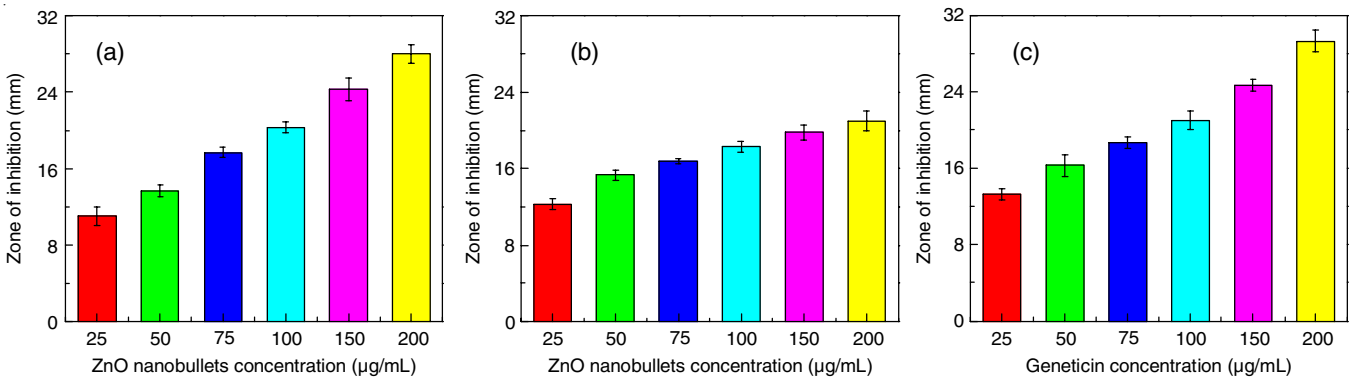

Fig. 5. Variation in ZOI with ZnO NBs concentrations in (a) well diffusion study and (b) disk diffusion study, (c) disc diffusion study showing the impact of Geneticin on *S. pombe*

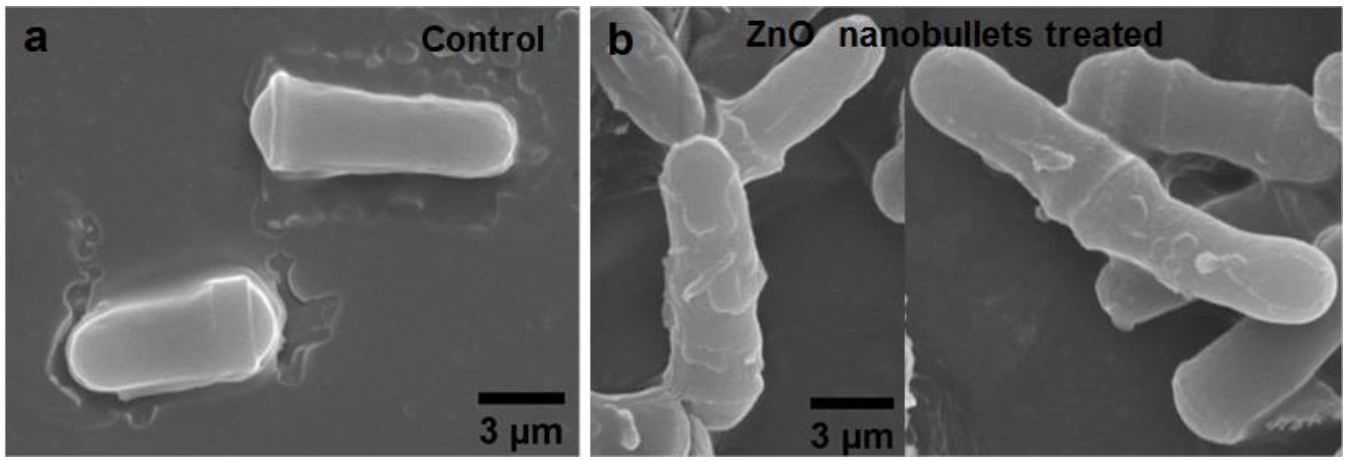

Fig. 6. SEM images of *S. pombe* (a) control, (b) ZnO NBs treated *S. pombe*

damage to the cell walls of *S. pombe*. The SEM micrograph of the untreated yeast cells showed rod-like shape with smooth surface (Fig. 6a), while cells with irregularities on their surface and damaged cell walls were observed in case of 200 µg/mL ZnO NBs treated *S. pombe* (Fig. 6b).

ROS generation in *S. pombe*: Since the formation of reactive oxygen species (ROS) has been hypothesized as a primary mechanism responsible for the antifungal effect of ZnO NBs against *S. pombe*, we sought to investigate its role and impact in order for better understanding of its orgins [30]. Thus, the effect of a known antioxidant N-acetyl-l-cysteine (NAC) on the growth of ZnO NBs treated *S. pombe* was studied. The antioxidant NAC has been shown to scavenge ROS [46,47] and thus is expected to decrease the antifungal action of ZnO NBs resulting in better growth of ZnO NBs treated *S. pombe*. Therefore, growth curve studies on *S. pombe* treated with 200 µg/mL ZnO NBs were carried out without or with NAC at 10, 20, 30, 40 and 50 mM. These experiments revealed an increased growth of 200 µg/mL ZnO NBs treated *S. pombe* when NAC concentration was increased from 10 to 50 mM (Fig. 7). These findings indicated that ROS generation has substantial contribution to the antifungal response of ZnO NBs.

Further, for direct quantification of the intracellular ROS level produced in *S. pombe* cells on treatment with ZnO NBs, a fluorescence assay [48] based on dye 2′,7′-dichlorodihydrofluorescein diacetate (H_2DCFDA) [49] was used. As shown in

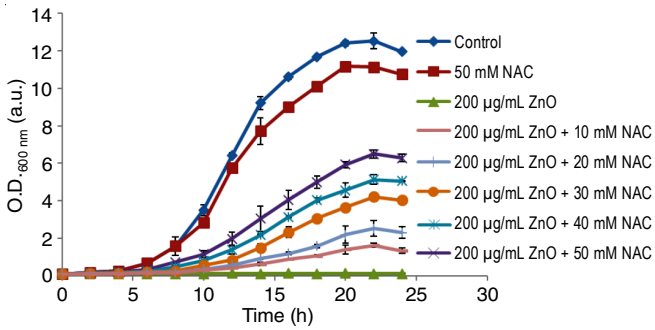

Fig. 7. Growth kinetics of ZnO NBs (200 µg/mL) treated *S. pombe* with or without NAC at different concentrations

Fig. 8a, 200 µg/mL ZnO NBs treated *S. pombe* cells stained with H_2DCFDA dye exhibited increased green fluorescence than the untreated *S. pombe* cells, which reveals an enhanced intracellular ROS formation. The adjusted mean fluorescence in 200 µg/mL ZnO NBs treated *S. pombe* was observed to be higher than the untreated cells and was comparable to the intracellular ROS generated in *S. pombe* on treatment with 10 mM H_2O_2 (Fig. 8b). Enhanced intracellular generation of ROS is clearly observed in 200 µg/mL ZnO NBs treated cells than the untreated yeast cells.

Membrane disintegration, protein leakage and DNA fragmentation: The impact of ZnO NBs on the integrity of the cell membrane of *S. pombe* utilizing Trypan blue dye exclusion

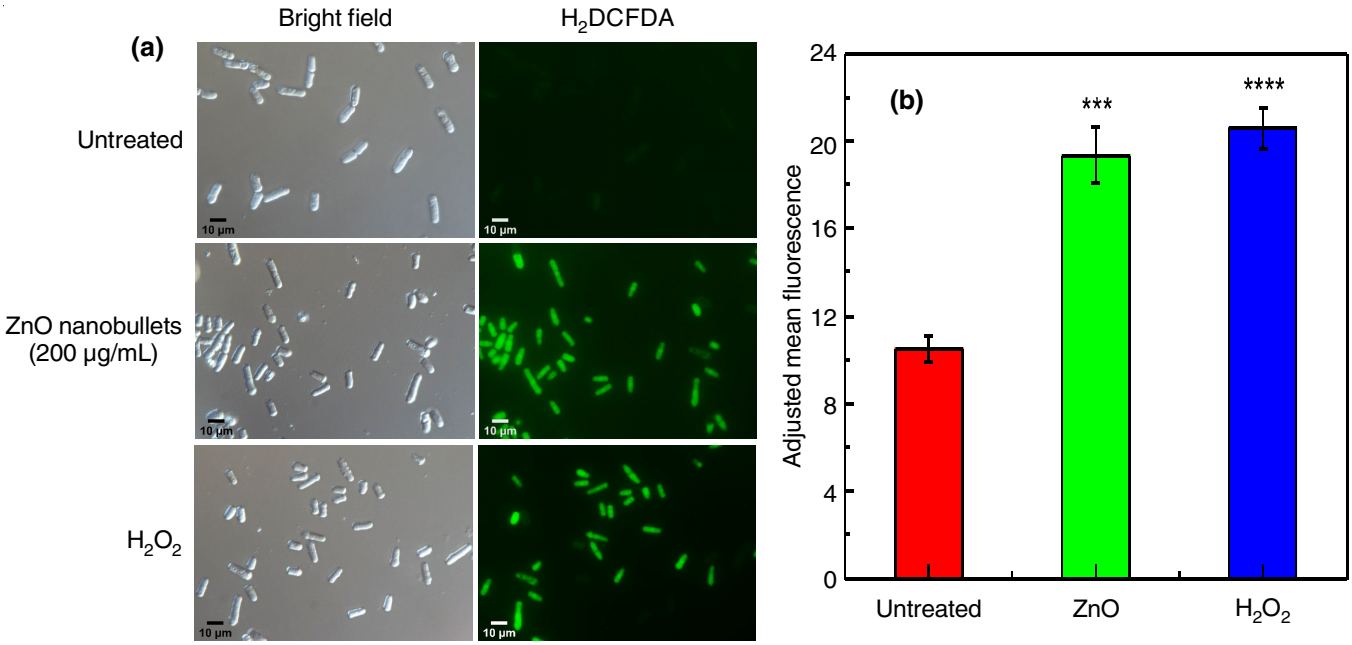

Fig. 8. (a) Fluorescence images of ZnO NBs treated *S. pombe* using H_2DCFDA dye. (b) Quantification of cellular ROS using adjusted mean fluorescence from two independent experiments. 200 cells of each sample were analyzed in each technical replicate. Average mean adjusted fluorescence was plotted with mean ± SD. *p*-values (**** = $p < 0.0001$, *** = $p < 0.001$) have also been included

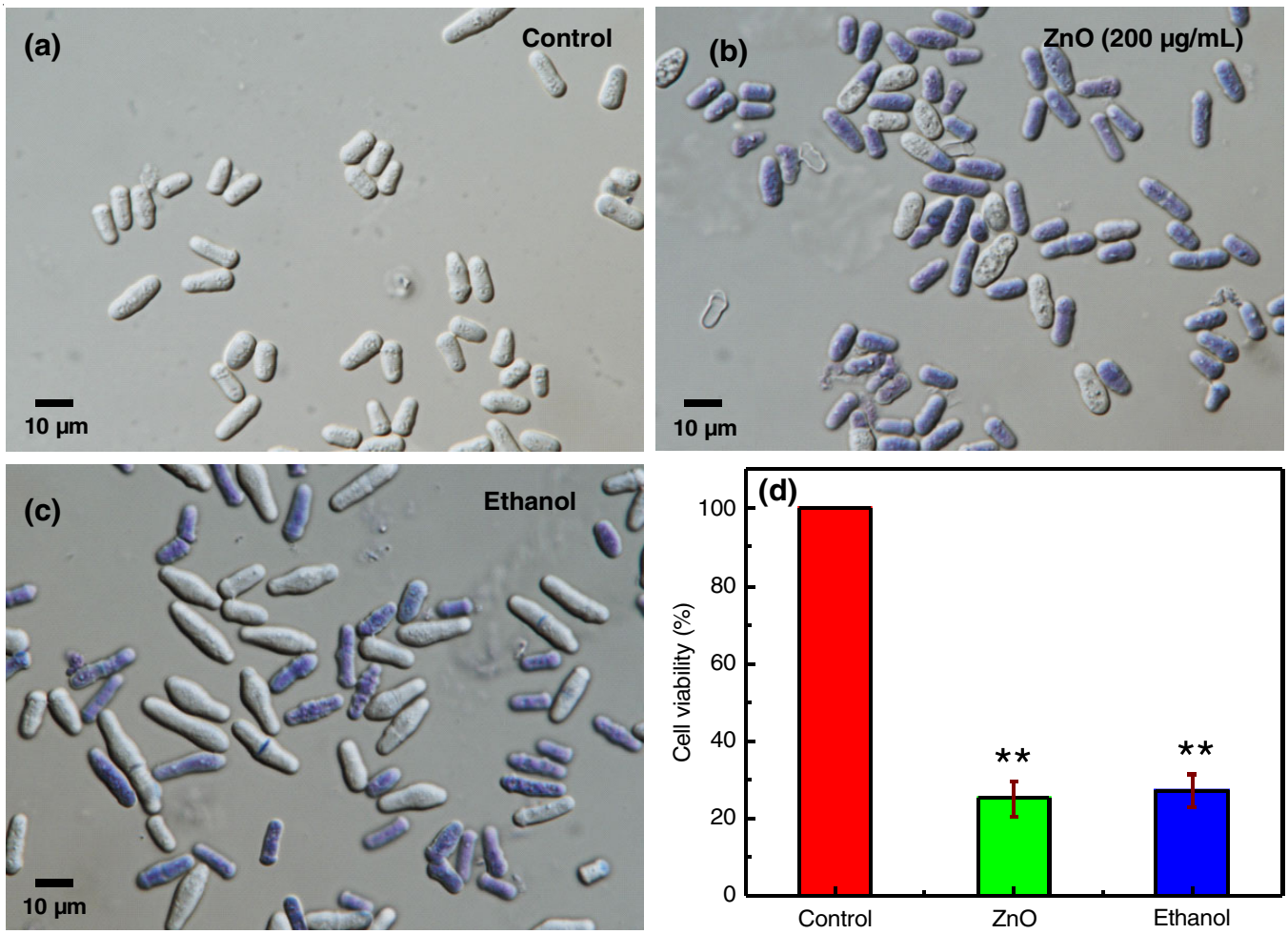

Fig. 9. (a) Optical images and (b) Cell viability percentage calculated from the Trypan blue assay. *S. pombe* were treated with 200 µg/mL ZnO NBs or ethanol and incubated at 32 °C for 2h. 200 cells were analyzed in each technical replicate. *p*-value (** = $p < 0.01$) has also been included

assay [50] was also investigated. Living cells with cell membrane intact exclude the Trypan blue, whereas dead cells take up the dye giving bluish colour to these cells. The optical micrographs of *S. pombe* treated for 2 h with either 200 µg/mL ZnO NBs or ethanol (as control), followed by staining with Trypan blue are shown in Fig. 9a. More the number of yeast cells were stained as blue in 200 µg/mL ZnO NBs treated yeast cells than the untreated yeast cells. The cell viability decreased to 24.99% for ZnO NBs treated yeastcells (Fig. 9b) and 27.28% for yeast cells treated with ethanol indicate that the treatment with ZnO NBs led to increased disintegration of cell membrane and thus decreased viability.

For protein leakage studies, the concentration protein in supernatant of ZnO NBs treated and untreated *S. pombe* cultures using Bradford assay was examined. Fig. 10 shows the results on ZnO NBs treated *S. pombe* at different concentration for 2 h. The protein concentration in the supernatants of *S. pombe* treated with 25, 50, 75, 100, 150 µg/mL ZnO NBs was estimated as 2.112 ± 0.086, 2.868 ± 0.053, 3.974 ± 0.334, 5.233 ± 0.297 and 5.862 ± 0.247 µg/mL, respectively. The concentration of protein in case of 200 µg/mL ZnO NBs treated cells was found to be 7.056 ± 0.328 µg/mL, which is 7.57 times larger than that for the untreated *S. pombe* cells (0.932 ± 0.148 µg/mL). This clearly indicates that damage to cell wall is caused by the treatment of *S. pombe* with ZnO NBs, subsequently resulting in substantial protein leakage.

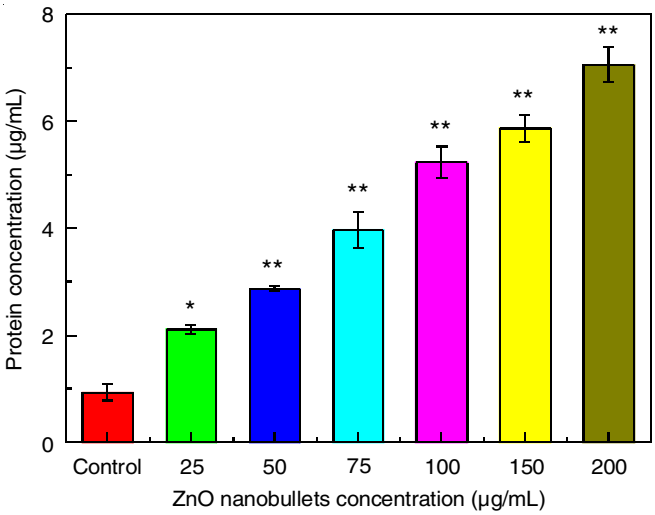

Fig. 10. Estimation of protein leakage. Varying ZnO NBs concentration were mixed with *S. pombe* cultures and protein concentration in supernatant was estimated by Bradford assay. Average values from three independent experiments (with 2 technical replicates each) has been plotted with SD. *p*-values (** = $p < 0.01$, * = $p < 0.05$) have been included

Finally, the impact of ZnO nanoparticles on the integrity of genomic DNA in *S. pombe* cells was also investigated. Isolation of genomic DNA from the *S. pombe* cells treated with 10 mM H_2O_2 (control) or 200 µg/mL ZnO NBs for 10 h and 15 h was carried out and then the genomic DNA was run on the agarose gel. Treatment of *S. pombe* cells with 10 mM H_2O_2 (control) or 200 µg/mL ZnO NBs led to a DNA fragmentation (Fig. 11). The untreated *S. pombe* cells did not exhibit any DNA fragmentation (Fig. 11). All the observations taken together suggest that the intracellular ROS produced by treatment with ZnO NBs lead to cell wall damage, protein leakage and DNA fragmentation in the *S. pombe*.

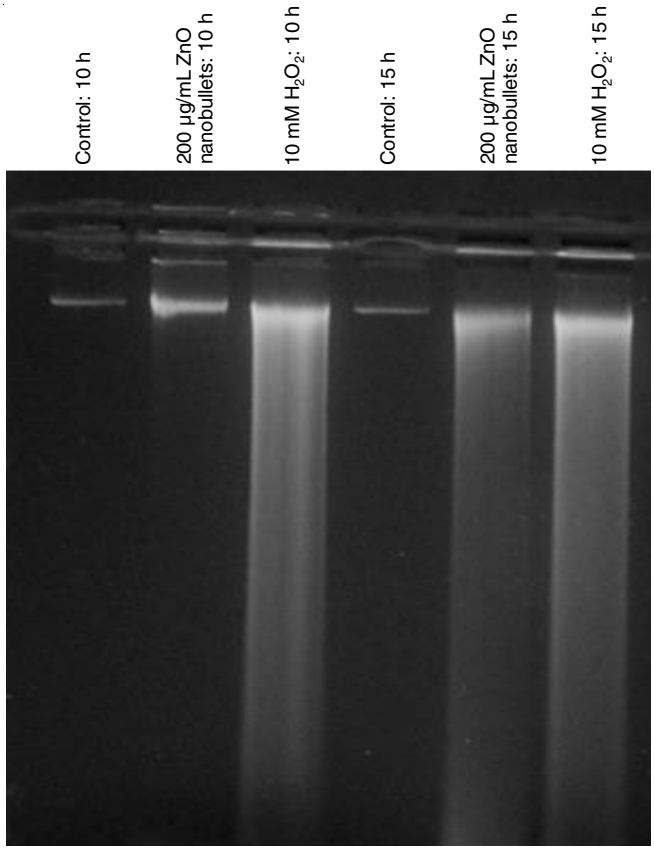

Fig. 11. DNA fragmentation in *S. pombe* upon treatment with ZnO NBs or 10 mM H_2O_2

Conclusion

In summary, ZnO nanobullets (NBs) with average size of 50 nm exhibit a strong antifungal action against *S. pombe*. The MIC of these ZnO NBs was found to be 200 µg/mL, which was found comparable to that of common antibiotic geneticin. Moreover, the MIC of these ZnO NBs was found to be lower than those displayed by reported ZnO nanoparticles. Different assays provide evidence that treatment of *S. pombe* with ZnO nanobullets led to an increased accumulation of ROS in *S. pombe*, which further resulted in cell wall damage, protein leakage and DNA fragmentation.

ACKNOWLEDGEMENTS

The author is thankful to Prof. N. Sharma for useful suggestions which helped to improve the work and S. Choudhary and V. Bhardwaj for help during the experiments. BM also acknowledges Guru Gobind Singh Indraprastha University for Indraprastha Research Fellowship (IPRF).

CONFLICT OF INTEREST

The author declares that there is no conflict of interests regarding the publication of this article.

REFERENCES

1. M.C. Fisher, D.A. Henk, C.J. Briggs, J.S. Brownstein, L.C. Madoff, S.L. McCraw and S.J. Gurr, *Nature*, **484**, 186 (2012); https://doi.org/10.1038/nature10947
2. J. Tanwar, S. Das, Z. Fatima and S. Hameed, *Interdiscip. Perspect. Infect. Dis.*, **2014**, 541340 (2014); https://doi.org/10.1155/2014/541340
3. L. Scorzoni, M.P. de Lucas, A.C. Mesa-Arango, A.M. Fusco-Almeida, E. Lozano, M. Cuenca-Estrella, M.J. Mendes-Giannini and O. Zaragoza, *PLoS One*, **8**, e60047 (2013); https://doi.org/10.1371/journal.pone.0060047
4. D.W. Warnock, *Med. Mycol.*, **44**, 697 (2006); https://doi.org/10.1080/13693780601009493
5. J. Abbas, G.P. Bodey, H.A. Hanna, M. Mardani, E. Girgawy, D. Abi-Said, E. Whimbey, R. Hachem and I. Raad, *Arch. Intern. Med.*, **160**, 2659 (2000); https://doi.org/10.1001/archinte.160.17.2659
6. P. Makvandi, C. Wang, E.N. Zare, A. Borzacchiello, L. Niu and F.R. Tay, *Adv. Funct. Mater.*, **30**, 1910021 (2020); https://doi.org/10.1002/adfm.201910021
7. A.R. Cruz-Luna, H. Cruz-Martínez, A. Vásquez-López and D.I. Medina, *J. Fungi*, **7**, 1033 (2021); https://doi.org/10.3390/jof7121033
8. Q. Sun, J. Li and T. Le, *J. Agric. Food Chem.*, **66**, 11209 (2018); https://doi.org/10.1021/acs.jafc.8b03210
9. V.F. Consolo, A. Torres-Nicolini and V.A. Alvarez, *Sci. Rep.*, **10**, 20499 (2020); https://doi.org/10.1038/s41598-020-77294-6
10. Y. Wei, S. Chen, B. Kowalczyk, S. Huda, T.P. Gray and B.A. Grzybowski, *J. Phys. Chem. C*, **114**, 15612 (2010); https://doi.org/10.1021/jp1055683
11. J.B. Wright, K. Lam, D. Hansen and R.E. Burrell, *Am. J. Infect. Control*, **27**, 344 (1999); https://doi.org/10.1016/S0196-6553(99)70055-6
12. K.J. Kim, W.S. Sung, B.K. Suh, S.K. Moon, J.S. Choi, J.G. Kim and D.G. Lee, *Biometals*, **22**, 235 (2009); https://doi.org/10.1007/s10534-008-9159-2
13. A. Reinhardt and I. Neundorf, *Int. J. Mol. Sci.*, **17**, 701 (2016); https://doi.org/10.3390/ijms17050701
14. J. Panyam and V. Labhasetwar, *Adv. Drug Deliv. Rev.*, **55**, 329 (2003); https://doi.org/10.1016/S0169-409X(02)00228-4
15. B. Mohapatra, S. Mohapatra and N. Sharma, *Ceram. Int.*, **49**, 20218 (2023); https://doi.org/10.1016/j.ceramint.2023.03.146
16. D. Campoccia, L. Montanaro and C.R. Arciola, *Biomaterials*, **34**, 8533 (2013); https://doi.org/10.1016/j.biomaterials.2013.07.089
17. S.C. De la Rosa-García, P. Martínez-Torres, S. Gómez-Cornelio, M.A. Corral-Aguado, P. Quintana and N.M. Gómez-Ortíz, *J. Nanomater.*, **2018**, 3498527 (2018); https://doi.org/10.1155/2018/3498527
18. M. Ali, X. Wang, U. Haroon, H.J. Chaudhary, A. Kamal, Q. Ali, M.H. Saleem, K. Usman, A. Alatawi, S. Ali and M.F.H. Munis, *Ecotoxicol. Environ. Saf.*, **233**, 113311 (2022); https://doi.org/10.1016/j.ecoenv.2022.113311
19. M.A. Gondal, A.J. Alzahrani, M.A. Randhawa and M.N. Siddiqui, *J. Environ. Sci. Health Part A*, **47**, 1413 (2012); https://doi.org/10.1080/10934529.2012.672384
20. B. Das, M.I. Khan, R. Jayabalan, S.K. Behera, S.-I. Yun, S.K. Tripathy and A. Mishra, *Sci. Rep.*, **6**, 36403 (2016); https://doi.org/10.1038/srep36403
21. L. He, Y. Liu, A. Mustapha and M. Lin, *Microbiol. Res.*, **166**, 207 (2011); https://doi.org/10.1016/j.micres.2010.03.003
22. C.O. Dimkpa, J.E. McLean, D.W. Britt and A.J. Anderson, *Biometals*, **26**, 913 (2013); https://doi.org/10.1007/s10534-013-9667-6
23. J. Li, H. Sang, H. Guo, J.T. Popko, L. He, J.C. White, O. Parkash Dhankher, G. Jung and B. Xing, *Nanotechnology*, **28**, 155101 (2017); https://doi.org/10.1088/1361-6528/aa61f3
24. A.M. González-Merino, A. Hernández-Juárez, R. Betancourt-Galindo, Y.M. Ochoa-Fuentes, L.A. Valdez-Aguilar and M.L. Limón-Corona, *J. Phytopathol.*, **169**, 533 (2021); https://doi.org/10.1111/jph.13023
25. P.A. Arciniegas-Grijalba, M.C. Patiño-Portela, L.P. Mosquera-Sánchez, J.A. Guerrero-Vargas and J.E. Rodríguez-Páez, *Appl. Nanosci.*, **7**, 225 (2017); https://doi.org/10.1007/s13204-017-0561-3
26. S. Djearamane, L.J. Xiu, L.S. Wong, R. Rajamani, S. Kayarohanam, D. Bharathi, A.E. De Cruz, A.K. Janakiraman, M. Aminuzzaman, L.H. Tey and S. Selvaraj, *Coatings*, **12**, 1864 (2022); https://doi.org/10.3390/coatings12121864
27. I. Galván-Márquez, M. Ghiyasvand, A. Massarsky, M. Babu, B. Samanfar, K. Omidi, T.W. Moon, M.L. Smith and A. Golshani, *PLoS One*, **13**, e0193111 (2018); https://doi.org/10.1371/journal.pone.0193111
28. S.M. Kamel, S.F. Elgobashy, R.I. Omara, A.S. Derbalah, M. Abdelfatah, A. El-Shaer, A.A. Al-Askar, A. Abdelkhalek, K.A. Abd-Elsalam, T. Essa, M. Kamran and M.M. Elsharkawy, *J. Fungi*, **8**, 911 (2022); https://doi.org/10.3390/jof8090911
29. N.S. Seddighi, S. Salari and A.R. Izadi, *IET Nanobiotechnol.*, **11**, 883 (2017); https://doi.org/10.1049/iet-nbt.2017.0025
30. A. Lipovsky, Y. Nitzan, A. Gedanken and R. Lubart, *Nanotechnology*, **22**, 105101 (2011); https://doi.org/10.1088/0957-4484/22/10/105101
31. F. Ghorbani, P. Gorji, M.S. Mobarakeh, H.R. Mozaffari, R. Masaeli and M. Safaei, *J. Nanomater.*, **2022**, 7255181 (2022); https://doi.org/10.1155/2022/7255181
32. H. Yin, L. Xu and N.A. Porter, *Chem. Rev.*, **111**, 5944 (2011); https://doi.org/10.1021/cr200084z
33. B. Mohapatra, S. Choudhary, S. Mohapatra and N. Sharma, *Mater. Today Commun.*, **34**, 105083 (2023); https://doi.org/10.1016/j.mtcomm.2022.105083
34. H. Shinto, M. Takiguchi, Y. Furukawa, H. Minohara, M. Kojima, C. Shigaki, Y. Hirohashi and H. Seto, *Adv. Powder Technol.*, **31**, 3686 (2020); https://doi.org/10.1016/j.apt.2020.06.043
35. B. Mohapatra and N. Sharma, *Mater. Today Commun.*, **34**, 106597 (2023); https://doi.org/10.1016/j.mtcomm.2023.106597
36. S.X.T. Liang, L.S. Wong, Y.M. Lim, P.F. Lee and S. Djearamane, *S. Afr. J. Chem. Eng.*, **34**, 63 (2020); https://doi.org/10.1016/j.sajce.2020.05.009
37. B. Jakic, M. Buszko, G. Cappellano and G. Wick, *PLoS One*, **12**, e0179383 (2017); https://doi.org/10.1371/journal.pone.0179383
38. R.A. McCloy, S. Rogers, C.E. Caldon, T. Lorca, A. Castro and A. Burgess, *Cell Cycle*, **13**, 1400 (2014); https://doi.org/10.4161/cc.28401
39. M.M. Bradford, *Anal. Biochem.*, **72**, 248 (1976); https://doi.org/10.1016/0003-2697(76)90527-3
40. I. Hagan, Fission Yeast: A Laboratory Manual (2016).
41. N. Pariona, F. Paraguay-Delgado, S. Basurto-Cereceda, J.E. Morales-Mendoza, L.A. Hermida-Montero and A.I. Mtz-Enriquez, *Appl. Nanosci.*, **10**, 435 (2020); https://doi.org/10.1007/s13204-019-01127-w
42. O. Lupan, G.A. Emelchenko, V.V. Ursaki, G. Chai, A.N. Redkin, A.N. Gruzintsev, I.M. Tiginyanu, L. Chow, L.K. Ono, B. Roldan Cuenya, H. Heinrich and E.E. Yakimov, *Mater. Res. Bull.*, **45**, 1026 (2010); https://doi.org/10.1016/j.materresbull.2010.03.027
43. B. Cao, W. Cai and H. Zeng, *Appl. Phys. Lett.*, **88**, 161101 (2006); https://doi.org/10.1063/1.2195694
44. C.H. Ahn, Y.Y. Kim, D.C. Kim, S.K. Mohanta and H.K. Cho, *J. Appl. Phys.*, **105**, 013502 (2009); https://doi.org/10.1063/1.3054175
45. B. Lin, Z. Fu and Y. Jia, *Appl. Phys. Lett.*, **79**, 943 (2001); https://doi.org/10.1063/1.1394173
46. D.K. Ban and S. Paul, *Appl. Biochem. Biotechnol.*, **173**, 155 (2014); https://doi.org/10.1007/s12010-014-0825-2
47. A. Lee, S. Lee, M. Lee, M. Nam, S. Lee, J. Choi, H. Lee, D. Kim and K. Hoe, *Toxicol. Sci.*, **161**, 171 (2018); https://doi.org/10.1093/toxsci/kfx208
48. S.L. Hempel, G.R. Buettner, Y.Q. O'Malley, D.A. Wessels and D.M. Flaherty, *Free Radic. Biol. Med.*, **27**, 146 (1999); https://doi.org/10.1016/S0891-5849(99)00061-1
49. X. Chen, Z. Zhong, Z. Xu, L. Chen and Y. Wang, *Free Radic. Res.*, **44**, 587 (2010); https://doi.org/10.3109/10715761003709802
50. W. Strober, *Curr. Protoc. Immunol.*, **111**, A3.B.1 (2015); https://doi.org/10.1002/0471142735.ima03bs111